

---

This is an electronic reprint of the original article.  
This reprint may differ from the original in pagination and typographic detail.

Rudel, Stefan S.; Deubner, H. Lars; Müller, Matthias; Karttunen, Antti J.; Kraus, Florian  
**Complexes featuring a linear  $[N\equiv U\equiv N]$  core isoelectronic to the uranyl cation**

*Published in:*  
Nature Chemistry

*DOI:*  
[10.1038/s41557-020-0505-5](https://doi.org/10.1038/s41557-020-0505-5)

Published: 01/10/2020

*Document Version*  
Peer-reviewed accepted author manuscript, also known as Final accepted manuscript or Post-print

*Please cite the original version:*  
Rudel, S. S., Deubner, H. L., Müller, M., Karttunen, A. J., & Kraus, F. (2020). Complexes featuring a linear  $[N\equiv U\equiv N]$  core isoelectronic to the uranyl cation. *Nature Chemistry*, 12(10), 962-967.  
<https://doi.org/10.1038/s41557-020-0505-5>

---

This material is protected by copyright and other intellectual property rights, and duplication or sale of all or part of any of the repository collections is not permitted, except that material may be duplicated by you for your research use or educational purposes in electronic or print form. You must obtain permission for any other use. Electronic or print copies may not be offered, whether for sale or otherwise to anyone who is not an authorised user.

1 **Complexes featuring a linear [N≡U≡N] core isoelectronic to the uranyl**  
2 **cation**

3

4 Stefan S. Rudel <sup>1</sup>, H. Lars Deubner <sup>1</sup>, Matthias Müller <sup>1</sup>, Antti J. Karttunen <sup>2</sup>, Florian Kraus <sup>1,\*</sup>

5 **1** Anorganische Chemie, Fluorchemie, Fachbereich Chemie, Philipps-Universität Marburg, Hans-  
6 Meerwein-Str. 4, 35032 Marburg, Germany

7 **2** Department of Chemistry and Materials Science, Aalto University 00076 Aalto, Finland

8

9 **Abstract**

10 The aqueous chemistry of uranium is dominated by the linear uranyl cation [UO<sub>2</sub>]<sup>2+</sup>, yet the isoelectronic  
11 nitrogen-based analogue of this ubiquitous cation, molecular [UN<sub>2</sub>], has so far only been observed in an  
12 argon matrix. Here, we present three different complexes of [UN<sub>2</sub>] obtained by the reaction of the  
13 uranium pentahalides UCl<sub>5</sub> or UBr<sub>5</sub> with anhydrous liquid ammonia. The [UN<sub>2</sub>] moieties are linear, with  
14 the U atoms coordinated by five additional ligands (ammonia, chloride or bromide), resulting in a  
15 pentagonal bipyramidal coordination sphere that is also commonly adopted by the uranyl cation  
16 [UO<sub>2</sub>(L)<sub>5</sub>]<sup>2+</sup>. In all three cases, the nitrido ligands are further coordinated through their lone pairs by the  
17 Lewis acidic ligands [U(NH<sub>3</sub>)<sub>8</sub>]<sup>4+</sup> to form almost linear, trinuclear complex cations. Those were  
18 characterized by single crystal X-ray diffraction, Raman and IR spectroscopy, <sup>14</sup>N/<sup>15</sup>N isotope studies,  
19 and quantum chemical calculations which support the presence of U≡N triple bonds within the [UN<sub>2</sub>]  
20 moieties.

21

22

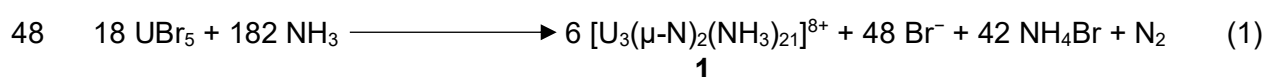
23 Although the uranyl cation  $[\text{UO}_2]^{2+}$  is a prevalent species in uranium chemistry, its isoelectronic nitrogen  
24 analogue  $[\text{UN}_2]$  has not been encountered yet outside an argon matrix, as NUN and NUNH species<sup>1-3</sup>.  
25 Under these conditions, several complexes of  $[\text{UN}_2]$  with one to five dinitrogen ligands,  $[\text{UN}_2(\text{N}_2)_x]$  ( $x$   
26 = 1 to 5), have also been observed.<sup>4</sup> Beyond the fundamental interest in these species, uranium nitrides  
27 are also investigated for their catalytic properties for example for  $\text{CO}_2$  or  $\text{N}_2$  activation, and as a future  
28 fuel in generation IV nuclear reactors as well as in space power and propulsion systems.<sup>5-13</sup>

29 The investigation of multiple bonding to uranium atoms is also a challenge for experimental and  
30 theoretical chemistry alike.<sup>14-16</sup> Previous works used very elaborate ligands to stabilize such compounds  
31 in order to counter the high reactivity of terminal uranium nitrides towards organic solvents and  
32 reagents.<sup>14,17,18</sup> Here we report on a  $[\text{UN}_2]$  fragment, a linear  $[\text{N}=\text{U}=\text{N}]$  moiety which is stabilized only  
33 by the coordination of two Lewis acidic ammine uranium(IV) cations, ammonia molecules, or halido  
34 ligands. These  $[\text{UN}_2]$ -containing species occur as metastable intermediates of the disproportionation and  
35 ammonolysis of the uranium pentahalides  $\text{UCl}_5$  and  $\text{UBr}_5$ . Choosing liquid ammonia as both reactant  
36 and solvent prevented side reactions leading to non-nitrogen based products from occurring — this  
37 circumstance is especially beneficial with regard to the synthesis of ceramic nuclear fuels, where carbide  
38 and oxide contamination is detrimental.<sup>10</sup>

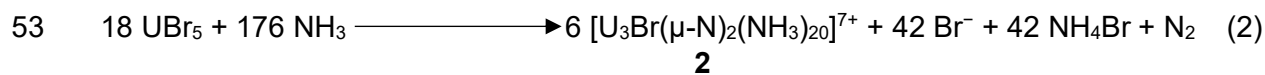
## 39 **Results and Discussion**

### 40 *Synthesis and structural description of the $[\text{UN}_2]$ complexes*

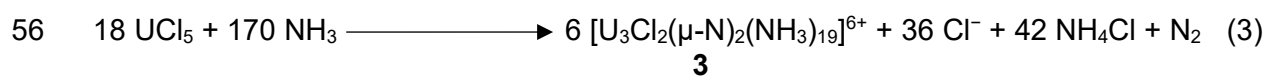
41 We reacted  $\text{UBr}_5$  with  $\text{NH}_3$  at  $-78\text{ }^\circ\text{C}$  and observed the formation of a yellow-green suspension along  
42 with a slight evolution of nitrogen gas. The compound  $[(\text{NH}_3)_8\text{U}(\mu\text{-N})(\text{NH}_3)_5\text{U}(\mu\text{-}$   
43  $\text{N})\text{U}(\text{NH}_3)_8]\text{Br}_8 \cdot 26\text{NH}_3$ ,  $(1\text{Br}_8 \cdot 26\text{NH}_3)$ , crystallized (idealized Eq. 1) after two weeks at  $-40\text{ }^\circ\text{C}$ . X-ray  
44 crystal structure determination under consistent cooling and strict exclusion of air showed a linear tri-  
45 nuclear uranium complex with N-bridged uranium atoms (Figure 1a) that are additionally coordinated  
46 by  $\text{NH}_3$  ligands. The central U atom ( $\text{U}_{\text{cen}}$ ) of the  $[\text{UN}_2]$  unit carries five ammine ligands whereas eight  
47 ammine ligands coordinate each of the terminal U atoms ( $\text{U}_{\text{ter}}$ ).



49 When we reacted  $\text{UBr}_5$  with anhydrous ammonia at room temperature in a sealed bomb tube, the  
 50 chemically related compound  $[(\text{NH}_3)_8\text{U}(\mu\text{-N})\text{Br}(\text{NH}_3)_4\text{U}(\mu\text{-N})\text{U}(\text{NH}_3)_8]_2\text{Br}_{14}\cdot 21\text{NH}_3$  ( $2\text{Br}_7\cdot 10.5\text{NH}_3$ )  
 51 was formed (idealized Eq. 2) as evidenced by single-crystal diffraction. In this compound, the central U  
 52 atom of the  $[\text{UN}_2]$  unit carries one bromido and four ammine ligands (Figure 1b).



54 A third similar,  $[\text{UN}_2]$  containing compound,  $[(\text{NH}_3)_8\text{U}(\mu\text{-N})\text{Cl}_2(\text{NH}_3)_3\text{U}(\mu\text{-N})\text{U}(\text{NH}_3)_8]\text{Cl}_6\cdot 6\text{NH}_3$ ,  
 55 ( $3\text{Cl}_6\cdot 6\text{NH}_3$ ), crystallized, when we reacted  $\text{UCl}_5$  with ammonia at room temperature (idealized Eq. 3).



57 Compound  $3\text{Cl}_6\cdot 6\text{NH}_3$  carries two chloride ligands and three ammine ligands at the U atom of the  $[\text{UN}_2]$   
 58 unit (Figure 1c).

59 Figure 1 shows the structure of the cations  $1^{8+}$ ,  $2^{7+}$ , and  $3^{6+}$  and some selected U–N distances observed  
 60 in their crystal structures. The total charge of the cations  $1^{8+}$ ,  $2^{7+}$ , and  $3^{6+}$  is dictated by the number of  
 61 counter-ions present in the structure. This requires a mixed valence for the three uranium atoms of each  
 62 complex cation. Regarding the differing lengths of the  $\text{U}_{\text{cen}}\text{--}(\mu\text{-N})\text{--}\text{U}_{\text{ter}}$  bonds, the only reasonable  
 63 assignment of oxidation numbers is +VI for the  $\text{U}_{\text{cen}}$  atom, and +IV for the terminally bound  $\text{U}_{\text{ter}}$  atoms.  
 64 In many nitrogen-bridged uranium complexes, the nitride ligand is stabilized to such an extent that the  
 65 compounds are better described as imides,  $\text{U}=\text{NR}$ , rather than  $\text{U}\equiv\text{N}$ .<sup>9,12,19,20</sup> In cation  $1^{8+}$ , the  $\text{U}_{\text{cen}}\text{--}(\mu\text{-N})$   
 66 bond lengths of 1.853(3) and 1.854(3) Å are of course longer than those calculated for molecular  
 67  $[\text{N}\equiv\text{U}\equiv\text{N}]$ ,  $[\text{NUN}(\text{N}_2)_5]$ , and  $[\text{N}\equiv\text{UF}_3]$  (1.717,<sup>21</sup> 1.753<sup>4</sup> and 1.759 Å,<sup>22</sup> respectively) but close to the  
 68 terminal  $\text{U(VI)}\equiv\text{N}$  triple bonds reported for  $[\text{U}(\text{N})(\text{N}(\text{CH}_2\text{NSi-Pr}_3)_3)]$  (1.799(7) Å). They are equal,  
 69 within the tripled standard uncertainty, to those in  $[\text{Na}(12\text{-crown-4})_2][\text{U}(\text{N})(\text{N}(\text{CH}_2\text{NSi-Pr}_3)_3)]$   
 70 (1.825(15) Å)<sup>14,18</sup> and considerably shorter than in  $(\text{C}_6\text{F}_5)_3\text{B}\text{--}\text{N}\equiv\text{U}(\text{N}[t\text{-Bu}](3,5\text{-Me}_2\text{C}_6\text{H}_3))_3$   
 71 (1.880(4) Å).<sup>23</sup> Consequently, the  $\text{U}_{\text{ter}}\text{--}(\mu\text{-N})$  distances of 2.304(3) and 2.300(3) Å are longer than in  
 72 single bonded uranium(IV) nitrido complexes like  $[(\text{C}_5\text{Me}_5\text{U}(\mu\text{-I})_2)_3\text{N}]$  (2.138(3) to 2.157(3) Å).<sup>24</sup>  
 73 Double bonded imido ligands typically show significantly longer  $\text{U}=\text{N}$  bonds (1.920(2) to 2.086 Å).<sup>25,26</sup>  
 74 Some uranyl-analogous diimido complexes exhibit extremely short U–N distances in the range of  
 75  $\text{U(VI)}\equiv\text{N}$  triple bonds, like 1.848(4) Å in  $[\text{U}(\text{N}t\text{-Bu})_2\text{I}_2(\text{THF})_2]$ .<sup>16</sup> This might be attributed to the small

76 coordination number of six and the relatively small ligands. The  $U_{\text{cen}}-(\mu\text{-N})-U_{\text{ter}}$  angles of cation  $\mathbf{1}^{8+}$   
77 are close to  $180^\circ$  ( $177.98(14)^\circ$  and  $178.44(17)^\circ$ ), as is the  $(\mu\text{-N})-U_{\text{cen}}-(\mu\text{-N})$  angle ( $179.07(11)^\circ$ ). This  
78 is expected for the species  $[\text{N}\equiv\text{U}\equiv\text{N}]$ . The pentagonal-bipyramidal coordination of the  $U_{\text{cen}}$  atom is also  
79 common in uranyl chemistry.<sup>16,27,28</sup> In light of this we interpret cation  $\mathbf{1}^{8+}$  with the Lewis structure  
80 depicted in Figure 1a. The central moiety represents the nitrido analogue of a pentaammine uranyl(VI)  
81 cation,  $[\text{UN}_2(\text{NH}_3)_5]$ , which is stabilized by the weaker coordination of two  $[\text{U}(\text{NH}_3)_8]^{4+}$  cations to the  
82 nitrido ligands.

83 Single crystals of the compound  $2\text{Br}_7 \cdot 10.5\text{NH}_3$  revealed the second example of such a cation. Their  
84 structure contains two symmetry-independent cations  $\mathbf{2}^{7+}$  shown in Figure 1b. In comparison to cation  
85  $\mathbf{1}^{8+}$ , a bromido ligand lowers the charge of the trinuclear complex to  $7+$  and displaces one of the five  
86 ammine ligands at the central U atom. Compared to the  $U_{\text{ter}}$  atoms, the  $U_{\text{cen}}$  atom is the chemically harder  
87 since higher valent atom and as such it is preferred by the bromido ligand. The  $U_{\text{cen}}-(\mu\text{-N})$  atom distances  
88 of cations  $\mathbf{2}^{7+}$  ( $1.799(8)$ ,  $1.870(9)$  Å, and  $1.816(9)$ ,  $1.851(10)$  Å) are in agreement to those of cations  $\mathbf{1}^{8+}$   
89 (and  $\mathbf{3}^{6+}$ ). The two crystallographically independent  $[\text{UN}_2]$  units are essentially linear with  $179.0(4)$  and  
90  $178.6(3)^\circ$ . The appendant  $U_{\text{cen}}-(\mu\text{-N})-U_{\text{ter}}$  angles deviate a little more from linearity with  $171.6(5)$  and  
91  $175.4(5)^\circ$ , and  $171.6(5)$  and  $174.1(6)^\circ$ , which is likely due to the steric demand of the bromido ligand.

92  $[(\text{NH}_3)_8\text{U}(\mu\text{-N})\text{Cl}_2(\text{NH}_3)_3\text{U}(\mu\text{-N})\text{U}(\text{NH}_3)_8]\text{Cl}_6 \cdot 6\text{NH}_3$ , ( $\mathbf{3Cl}_6 \cdot 6\text{NH}_3$ ) is the third example of a  $[\text{UN}_2]$   
93 complex. Compared to cation  $\mathbf{1}^{8+}$ , two ammine ligands of the  $U_{\text{cen}}$  atom are replaced by chlorido ligands  
94 (Figure 1c), lowering the total charge of the complex to  $6+$ . Expectedly, the hard  $\text{Cl}^-$  anion preferably  
95 coordinates to the chemically harder  $U_{\text{cen}}$  atom. For other examples of this coordination behavior see the  
96 literature.<sup>27</sup> The  $U_{\text{cen}}-(\mu\text{-N})$  atom distances of  $\mathbf{3}^{6+}$  ( $1.834(5)$  and  $1.853(5)$  Å) are equal within the doubled  
97 standard uncertainty. The appendant  $U_{\text{cen}}-(\mu\text{-N})-U_{\text{ter}}$  angles however are with  $170.9(3)$  and  $172.4(3)^\circ$   
98 slightly smaller compared to those in cation  $\mathbf{1}^{8+}$ , which we attribute to the steric demand of the bound  
99 Cl atoms. The U–Cl atom distances ( $2.837(1)$  and  $2.807(1)$  Å) in cation  $\mathbf{3}^{6+}$  are considerably longer than  
100 in  $[(\text{py})_3\text{UO}_2\text{Cl}_2]$  ( $2.693(1)$  and  $2.734(1)$  Å),<sup>28</sup> which is attributed to the higher covalence of the U–N  
101 bond in comparison to the U–O bond. However, the Cl–U–Cl angle ( $149.99(4)^\circ$ ) of cation  $\mathbf{3}^{6+}$  is still  
102 comparable to the corresponding angle of  $[(\text{py})_3\text{UO}_2\text{Cl}_2]$  ( $146.80(4)^\circ$ ).<sup>28</sup> Supplementary Table 1 holds  
103 selected crystallographic data and details of the structure determinations of the title compounds.

104 For the reaction mechanism, we propose that a dissolved U(V) species disproportionates in ammonia to  
105 U(IV) and U(VI) species. It seems like some ammonia is oxidized by such a U(VI) species to N<sub>2</sub>, while  
106 formation of the trinuclear U complexes that we observe in the solid-state proceeds via deprotonation  
107 of ammine ligands. Obviously, the nitrido ligands stabilize the central U(VI) species, while the nitrido  
108 complexes become stabilized by the coordination of [U(NH<sub>3</sub>)<sub>8</sub>]<sup>4+</sup> complexes.

### 109 *Crystal-chemical considerations*

110 The very oxophilic nature of uranium could undoubtedly lead to oxygen-containing compounds during  
111 the syntheses and the distinction of nitrogen and oxygen atoms in an X-ray experiment is usually  
112 regarded as difficult due to the similar atomic form factors. So, one could argue that not [UN<sub>2</sub>] but  
113 [UO<sub>2</sub>]<sup>2+</sup> or [UO<sub>2</sub>]<sup>+</sup> complexes were obtained instead. Besides our Raman spectroscopic evidence (v.i.)  
114 that shows the lack of U–O stretching vibrations but instead a clear isotope shift for a <sup>15</sup>NH<sub>3</sub> enriched  
115 compound, and the compliance with our quantum chemical structure optimizations (v.i.), also the crystal  
116 structure refinements show differences suitable to distinguish N from O atoms in these cases. A first  
117 substantial argument is the number of anions in the unit cell, dictating the total charge of the uranium  
118 complexes as **1**<sup>8+</sup>, **2**<sup>7+</sup>, and **3**<sup>6+</sup>. If the μ-bridging atoms were O atoms, all the U atoms would have to be  
119 in equal oxidation state (+IV). However, the highly asymmetric position of the bridging atoms between  
120 the U<sub>cen</sub> and the U<sub>ter</sub> atoms does not correspond to such a model and is additionally in stark contrast with  
121 usual U–O bond lengths in other molecular μ-O-bridged uranium complexes, where roughly symmetric  
122 bonds with distances around 2.1 Å are encountered.<sup>29–31</sup> However, in our cases we observe atom  
123 distances of circa 1.85 Å to the U<sub>cen</sub> and circa 2.3 Å to the U<sub>ter</sub> atoms. In consequence, we would have  
124 to have overlooked additional anions, or the oxidation states of some U<sub>ter</sub> atoms would have to be lower  
125 if [UO<sub>2</sub>]<sup>2+</sup> or [UO<sub>2</sub>]<sup>+</sup> cations were present. While additional bromide or chloride anions would  
126 undoubtedly be hard to overlook in X-ray crystal structure analyses of this type, one could argue that X-  
127 ray diffraction does not allow to distinguish ammonia of crystallization from amide anions or ammonium  
128 cations, especially if the H atoms of those species cannot be located. In consequence our assignments of  
129 charges of the cations and the oxidation states of the U atoms would be wrong. However, “free”, non-  
130 coordinating amide anions in the crystal structure can easily be ruled out. As previously reported, NH<sub>2</sub><sup>–</sup>

131 anions are much stronger ligands than  $\text{NH}_3$ ,  $\text{Cl}^-$ , and  $\text{Br}^-$  ligands, so that amide ions would coordinate  
132 to uranium atoms and could be distinguished from  $\text{NH}_3$  ligands by distinctly shorter U–N distances.<sup>27</sup>  
133 If the oxidation states of the  $\text{U}_{\text{cen}}$  atoms in the nitride-bridged cations would be lower than stated above,  
134 then additional  $\text{NH}_4^+$  cations would have to be present. However, ammonium cations in ammoniates are  
135 usually surrounded by ammonia molecules in the form of  $[\text{NH}_4(\text{NH}_3)_x]^+$  complexes ( $x = 1$  to 4).<sup>32–36</sup> The  
136  $\text{NH}_4^+\cdots\text{NH}_3$  hydrogen bonds in such  $[\text{NH}_4(\text{NH}_3)_x]^+$  cations are significantly shorter than hydrogen bonds  
137 between ammonia molecules of crystallization. To the best of our knowledge, every reported crystal  
138 structure containing  $[\text{NH}_4(\text{NH}_3)_x]^+$  cations, shows  $\text{NH}_4^+\cdots\text{NH}_3$  distances in a range from 2.8 to 2.9 Å.<sup>32–</sup>  
139 <sup>36</sup> The absence of such short N $\cdots$ N distances between nitrogen atoms that are not coordinating to U  
140 atoms in compounds  $\mathbf{1Br}_8\cdot 26\text{NH}_3$ ,  $\mathbf{2Br}_7\cdot 10.5\text{NH}_3$ , and  $\mathbf{3Cl}_6\cdot 6\text{NH}_3$  indicates the absence of  $\text{NH}_4^+$  cations  
141 in their crystal structures and our assignments of oxidation states given above appear reasonable.  
142 Furthermore, lower oxidation states for uranium than +IV in the complexes are highly unlikely, as the  
143 starting materials are the halides of U(V) and uranium(IV) compounds are thermodynamically stable in  
144 liquid ammonia under the applied conditions. So, further reduction to U(III) will not occur without an  
145 additional reducing agent.<sup>27</sup>  
146 Additional support is given by the isotropic displacement parameters ( $U_{\text{iso}}$ ) of the  $\mu$ -bridging N atoms  
147 which are similar to those of the other N atoms (ammine ligands) in the crystal structures with circa 0.02  
148 in cations  $\mathbf{1}^{8+}$  and  $\mathbf{2}^{7+}$ , and for  $\mathbf{3}^{6+}$  with circa 0.013. This indicates that their assignment as N atoms is  
149 plausible (see also Supplementary Table 2). If we change the atom assignment for the  $\mu$ -bridging atoms  
150 to O, their isotropic displacement parameters increase to circa 0.03 for  $\mathbf{1Br}_8\cdot 26\text{NH}_3$ , to circa 0.03 to 0.04  
151 for  $\mathbf{2Br}_7\cdot 10.5\text{NH}_3$ , and for  $\mathbf{3Cl}_6\cdot 6\text{NH}_3$  to 0.02, which does not compare with the other N atoms; it should,  
152 however, as O and N have rather similar atomic form factors. This indicates that less electron density  
153 than from an O atom occupies the  $\mu$ -bridging positions. That is, the atom assignment as N instead of O  
154 is more plausible. Additionally, the  $\mu$ -bridging N atoms are tightly bound in between the  $\text{U}_{\text{cen}}$  and  $\text{U}_{\text{ter}}$   
155 atoms, so their displacement ellipsoids should be slightly smaller in comparison to N atoms of ammonia  
156 molecules of solvation which are less tightly bound in the crystal structure. This is observed for the  $\mu$ -  
157 bridging atoms being N atoms, but not if they are replaced by O atoms. If we use  $\mu$ -bridging O atoms  
158 and freely refine their site occupancy factors (SOF), they become smaller (see Supplementary Table 2)

159 and deviate much more from unity in comparison. This also indicates that less electron density must  
160 occupy this position, so the assignment of the  $\mu$ -bridging atoms as N instead of O is better.

161

### 162 *Raman spectroscopic investigations and $^{15}\text{N}$ labeling studies*

163 The sensitivity of compounds  $1\text{Br}_8 \cdot 26\text{NH}_3$ ,  $2\text{Br}_7 \cdot 10.5\text{NH}_3$  and  $3\text{Cl}_6 \cdot 6\text{NH}_3$  against air and moisture and  
164 especially their rapid decomposition at temperatures above the boiling point of ammonia – if not under  
165 pressurized ammonia – prevented many analyses, as at least the transfer of a compound into most  
166 analytical instruments must happen at room temperature. However, we were able to obtain Raman  
167 spectra in situ by using thin-walled fused silica ampoules as reaction vessels. All spectra of compounds  
168  $1\text{Br}_8 \cdot 26\text{NH}_3$  and  $3\text{Cl}_6 \cdot 6\text{NH}_3$  (Extended Data Fig. 1) show bands in the region of 888 to 955  $\text{cm}^{-1}$ , which  
169 can be assigned to the  $\text{U}\equiv\text{N}$  stretching vibrations of triple bonded uranium nitrides. Organic imido  
170 complexes usually show absorption in the 1200  $\text{cm}^{-1}$  region, which however is a coupling of the UN  
171 and NC resonance.<sup>16</sup> The  $\text{U}=\text{NH}$  stretch in  $\text{N}\equiv\text{U}=\text{N}-\text{H}$  is observed at 752  $\text{cm}^{-1}$ .<sup>2</sup>

172 Crystals of  $1\text{Br}_8 \cdot 26\text{NH}_3$  grown at  $-40\text{ }^\circ\text{C}$ , as well as their surrounding powder, show a main band at 936  
173  $\text{cm}^{-1}$  and two smaller bands at 876 and 955  $\text{cm}^{-1}$  (Extended Data Fig. 1). The main band is in accordance  
174 with the terminal nitrides  $[\text{NUF}_3]$  (937  $\text{cm}^{-1}$ ) and  $[\text{UN}(\text{N}(\text{CH}_2\text{CH}_2\text{NSi-Pr}_3)_3)][\text{Na}(12\text{-crown-4})_2]$  (936  
175  $\text{cm}^{-1}$ ), while a band at 955  $\text{cm}^{-1}$  was reported for  $[\{\text{U}(\mu\text{-N})(\mu\text{-Na})(\text{N}(\text{CH}_2\text{CH}_2\text{NSi-Pr}_3)_3)\}_2]$ , which is  
176 close to the 966  $\text{cm}^{-1}$  stretch of  $[\text{N}\equiv\text{U}=\text{N}-\text{H}]$ .<sup>2,18,22</sup> The  $\text{U}\equiv\text{N}$  stretch of  $[\text{UN}(\text{N}(\text{CH}_2\text{CH}_2\text{NSi-Pr}_3)_3)]$  was  
177 observed at 914  $\text{cm}^{-1}$ .<sup>14</sup> Four bands at 3145, 3213, 3291 and 3347  $\text{cm}^{-1}$  can be assigned to the NH stretch  
178 of the ammine ligands.<sup>37</sup> Raman spectra of the mother liquor of  $1\text{Br}_8 \cdot 26\text{NH}_3$  show a single band in the  
179  $\text{U}\equiv\text{N}$  region at 888  $\text{cm}^{-1}$  (Extended Data Fig. 1). We assign this to a strong U–N interaction that is  
180 weakened in comparison with the one in cation  $\mathbf{1}^{8+}$ . However, the actual species present in solution  
181 remains unknown.

182 Our simulated Raman spectra for the isolated cations show the symmetric stretching vibration of the  
183  $\text{U}\equiv\text{N}$  triple bonds of cation  $\mathbf{1}^{8+}$  (Extended Data Fig. 2) at 950  $\text{cm}^{-1}$  and for free, gas-phase  $[\text{UN}_2]$  at 1117  
184  $\text{cm}^{-1}$ . The deviation compared with the experimental value for the  $[\text{NUN}]$  molecule inside an argon  
185 matrix (1051  $\text{cm}^{-1}$ ) is due to additional ligands binding to the  $\text{U}_{\text{cen}}$  atom, as also observed for the matrix-



186 isolated  $[\text{UN}_2(\text{N}_2)_x]$  complexes ( $x = 1$  to  $5$ ).<sup>3,4</sup> Additionally, the matrix effect and the harmonic  
187 approximations used in the calculations lead to deviations.<sup>1</sup> Naturally, all  $[\text{UN}_2]$  molecules coordinated  
188 by additional ligands will show bands at lower wavenumbers in comparison to an isolated  $[\text{N}\equiv\text{U}\equiv\text{N}]$   
189 molecule.

190 We performed isotope labeling studies and obtained the compounds  $2\text{Br}_7 \cdot 10.5\text{NH}_3$  with natural  $^{14}\text{N}/^{15}\text{N}$   
191 isotope ratio, and  $2\text{Br}_7 \cdot 10.5^{15}\text{NH}_3$  using  $^{15}\text{N}$  enriched ammonia. The lattice parameters of both  
192 compounds were very similar (see Supplementary Table 1) which shows that we obtained identical  
193 compounds except for the  $^{15}\text{N}$  enrichment. Thus, a direct comparison of the Raman spectra of the  
194 compound with natural  $^{14}\text{N}/^{15}\text{N}$  isotope ratio with the  $^{15}\text{N}$  enriched compound became possible (Figure  
195 2). While the band positions of the N–H stretch vibrations are virtually unchanged by the isotope  
196 substitution and are observed in the expected range from circa 3158 to 3380  $\text{cm}^{-1}$ , the band assigned to  
197 the U–N stretch vibration of the central  $[\text{UN}_2]$  unit, is shifted from 906 to 883  $\text{cm}^{-1}$  upon  $^{15}\text{N}$  isotope  
198 labeling. The isotope shift is circa  $-23 \text{ cm}^{-1}$ , the ratio is 1.026. This value agrees excellently with matrix  
199 studies on  $[\text{U}^{14}\text{N}_2]$  and  $[\text{U}^{15}\text{N}_2]$ , where a shift of  $-22.6 \text{ cm}^{-1}$  was reported.<sup>1</sup> In nitrido complexes of iron,  
200 also  $-23 \text{ cm}^{-1}$  were observed,<sup>38</sup> while matrix isolation studies on dinitrogen complexes of  $[\text{UN}_2]$  showed  
201 a shift of  $-31 \text{ cm}^{-1}$  with a ratio of 1.031. As shown below, our quantum chemical calculations for cation  
202  $2^{7+}$  lead, due to the harmonic approximation, to a slightly larger isotope shift of  $-32 \text{ cm}^{-1}$  with a ratio of  
203 1.035. Our Raman measurements confirm also the absence of O atoms, e.g. in the form of  $[\text{UO}_2]^{2+}$  ions,  
204 as then additional U–O bands or no isotope shift would have been observed.

#### 205 *Effects of prolonged storage and room-temperature decomposition*

206 Prolonged storage of compounds  $1\text{Br}_8 \cdot 26\text{NH}_3$  and  $3\text{Cl}_6 \cdot 6\text{NH}_3$  (see below) in liquid ammonia for several  
207 weeks shows them to be only metastable, even at  $-40 \text{ }^\circ\text{C}$ . Both decompose to a pale-yellow powder.  
208 From the remains of compound  $1\text{Br}_8 \cdot 26\text{NH}_3$  the yellow uranium(IV) compound  $[\text{U}(\text{NH}_3)_{10}]\text{Br}_4 \cdot 9\text{NH}_3$   
209 crystallized,<sup>27</sup> and  $\text{NH}_4\text{Br}$  and  $\text{NH}_4\text{Cl}$ , respectively, are present in the decomposition products after  
210 evaporation of the solvent ammonia at room temperature. The IR spectra (Extended Data Fig. 3) of these  
211 decomposition products show bands assigned to coordinated  $\text{NH}_3$  but no signs of any oxidic or  $[\text{UO}_2]^{2+}$   
212 impurities ( $\nu_{\text{as}}(\text{UO}_2^{2+})$ :  $\sim 911 - 960 \text{ cm}^{-1}$ ).<sup>39</sup> Bands at 769 and 842  $\text{cm}^{-1}$ , which would be in the range

213 assigned to the stretching frequency of  $[\text{UO}_2]^+$  ( $\sim 797 \text{ cm}^{-1}$ ),<sup>40</sup> appear only in the spectrum of the leftovers  
214 of  $1\text{Br}_8 \cdot 26\text{NH}_3$ . During the Raman measurement at room temperature under pressurized liquid ammonia,  
215 crystals of  $1\text{Br}_8 \cdot 26\text{NH}_3$  irreversibly decompose and recrystallize to an unknown compound that shows  
216 a single band at  $895 \text{ cm}^{-1}$  (Supplementary Figure 1), which is still in the range of strong U–N  
217 interactions. The Raman spectrum of the surrounding powder reveals a mixture of  $1\text{Br}_8 \cdot 26\text{NH}_3$  and the  
218 unknown decomposition product. Compound  $3\text{Cl}_6 \cdot 6\text{NH}_3$  generates a similar spectrum with a major band  
219 at  $887 \text{ cm}^{-1}$ , a small band at  $913 \text{ cm}^{-1}$  and the U–Cl stretch at  $357 \text{ cm}^{-1}$ . The calculated value for the  
220 symmetric stretch of the  $\text{U}\equiv\text{N}$  triple bonds in cation  $3^{6+}$  (Extended Data Fig. 2) is  $969 \text{ cm}^{-1}$ . The  
221 deviations are due to the measurement on the solid compounds at room temperature in contrast to the  
222 calculations of the cations in the gas phase at 0 K within the harmonic approximation.

### 223 *Powder X-ray diffraction study of the decomposition product*

224 For an additional indication of the absence of O atoms within the compounds presented here, the room  
225 temperature residue of compound  $1\text{Br}_8 \cdot 26\text{NH}_3$  was heated inside a welded steel ampoule under argon to  
226  $600 \text{ }^\circ\text{C}$  and cooled down to room temperature.  $\text{UNBr}^{41,42}$  and  $\text{UBr}_3$  were formed as the main products as  
227 was shown by powder X-ray diffraction analysis (Extended Data Fig. 4). If O atoms in form of uranyl  
228 ions would have been present in  $1\text{Br}_8 \cdot 26\text{NH}_3$ , then  $\text{UO}_2$  or  $\text{UO}_{2+x}$  should have been formed during  
229 heating in an amount of approximately 30 %, which could not have been overlooked by powder X-ray  
230 diffraction. We observe additional reflections of an unknown crystalline phase, which can neither be  
231 assigned to any known uranium oxide nor to any known uranyl compound: The strongest additional  
232 reflection at  $14.1^\circ 2\theta$  (Extended Data Fig. 4) is not matched by any known U–O-phase, while the  
233 reflection at circa  $28.6^\circ 2\theta$  could belong to the strongest reflection of  $\text{UO}_{2+x}$ -phases ( $x < 1$ ). However,  
234 the next strongest reflections of these phases are not observed in our powder pattern and therefore we  
235 deem their presence unlikely.

### 236 *Quantum chemical calculations*

237 Quantum chemical structure optimizations reproduce the structural motives observed in the solid state  
238 (hybrid density functional theory, DFT, see Methods). The calculated  $\text{U}_{\text{cen}}\equiv\text{N}$  distances for cations  $1^{8+}$ ,  
239  $2^{7+}$ , and  $3^{6+}$  (1.83, 1.82, and 1.82 Å, respectively) are only slightly smaller than the observed ones

240 (Supplementary Table 3) but longer than those calculated for free  $[N\equiv U\equiv N]$  (1.71 Å). This is attributed  
241 to the additional ammine, bromido and chlorido ligands, respectively, in cations  $\mathbf{1}^{8+}$ ,  $\mathbf{2}^{7+}$ , and  $\mathbf{3}^{6+}$  as can  
242 be shown by comparison with a hypothetical  $[UN_2(NH_3)_5]$  complex, which is analogous to the known  
243  $[UO_2(NH_3)_5]^{2+}$  cation.<sup>27</sup> Here, the  $U\equiv N$  distance increases to 1.77 Å, which is much closer to the  
244 distances observed in cations  $\mathbf{1}^{8+}$ ,  $\mathbf{2}^{7+}$ , and  $\mathbf{3}^{6+}$ . This is compliant with the elongated  $U\equiv N$  distance in  
245 matrix isolated  $[UN_2(N_2)_5]$ .<sup>4</sup> We investigated the bonding in the cations by using Intrinsic Bond Orbitals  
246 (IBOs, see Methods) (Figure 3 and Extended Data Fig. 5).<sup>43</sup> The IBOs of the  $[UN_2]$  moiety of cation  $\mathbf{1}^{8+}$   
247 (Figure 3) prove to be very similar to free  $[UN_2]$  and the  $U_{cen}$  contribution is only slightly lessened due  
248 to the coordination of the five ammine ligands. With two  $\sigma$ - and four  $\pi$ -bonds, we propose the  
249 formulation of the  $[UN_2]$  species as  $[N\equiv U\equiv N]$ . The IBO analysis of free  $[UN_2]$  is in line with the  
250 canonical molecular orbital analysis presented for  $[UN_2]$  previously.<sup>2,44,45</sup>

251 While the Lewis structure is consistent with that of the uranyl ion,  $[O\equiv U\equiv O]^{2+}$ , the differences in  
252 electronegativity of N and O influence the extent of covalence of the triple bonding. The bonding  
253 analysis (Supplementary Table 4) shows the bonds in free  $[UN_2]$  to be the most covalent. The ionic  
254 character of the  $U\equiv X$  triple bonds ( $X = N, O$ ) increases from  $[UN_2(NH_3)_5]$  over cations  $\mathbf{1}^{8+}$ ,  $\mathbf{2}^{7+}$ , and  $\mathbf{3}^{6+}$ ,  
255 to free  $[UO_2^{2+}]$  and  $[UO_2(NH_3)_5]^{2+}$ , as the contribution of the U atom to the  $\sigma$ - and  $\pi$ -orbitals decreases  
256 in this order. The Intrinsic Atomic Orbital (IAO) partial charges of free  $[UN_2]$  are in agreement with the  
257 CASSCF Mulliken partial charges reported previously.<sup>2</sup> The U atoms of cations  $\mathbf{1}^{8+}$ ,  $\mathbf{2}^{7+}$ , and  $\mathbf{3}^{6+}$   
258 naturally carry a higher partial charge compared with neutral  $[UN_2(NH_3)_5]$ . However, despite their  
259 oxidation state of +VI, the  $U_{cen}$  atoms only carry partial charges of +0.78, +0.72 and +0.70, respectively,  
260 as a result of the covalent character of the  $U\equiv N$  triple bonds. The IBOs (Extended Data Fig. 5) indicate  
261 a  $U_{ter}-(\mu-N)$  interaction which is similar to the  $U-NH_3$  contacts. This is represented by the dative single  
262 bonds in the Lewis pictures given in Figure 1).

## 263 Conclusion

264 The  $[UN_2]$  molecule is the isoelectronic analogue of the uranyl cation  $[UO_2]^{2+}$  and was observed for the  
265 first time outside matrix conditions. From reactions of  $UCl_5$  and  $UBr_5$  in liquid anhydrous ammonia we  
266 obtained the three compounds  $\mathbf{1}Br_8\cdot 26NH_3$ ,  $\mathbf{2}Br_7\cdot 10.5NH_3$ , and  $\mathbf{3}Cl_6\cdot 6NH_3$ . The linear  $[UN_2]$  molecules

267 are contained in the center of the trinuclear complex cations  $\mathbf{1}^{8+}$ ,  $\mathbf{2}^{7+}$ , and  $\mathbf{3}^{6+}$  and their U atoms are  
268 additionally coordinated by five ligands  $[\text{UN}_2(\text{NH}_3)_{5-x}\text{L}_x]^{x-}$  with  $x = 0$  for  $\mathbf{1}^{8+}$ ,  $x = 1$  and  $L = \text{Br}$  for  $\mathbf{2}^{7+}$ ,  
269 and  $x = 2$  and  $L = \text{Cl}$  for  $\mathbf{3}^{6+}$ . Additionally, the N atoms of the  $[\text{N}\equiv\text{U}\equiv\text{N}]$  moiety are coordinated by  
270  $[\text{U}(\text{NH}_3)_8]^{4+}$  units to form the trinuclear cations  $[(\text{H}_3\text{N})_8\text{U}-\{\text{UN}_2(\text{NH}_3)_{5-x}\text{L}_x\}-\text{U}(\text{NH}_3)_8]^{(8-x)+}$ . Structural,  
271 crystal-chemical, and crystallographic considerations as well as powder X-ray diffraction analysis on  
272 annealed samples suggest the absence of O-containing species, such as  $[\text{UO}_2]^{2+}$  or  $[\text{UO}_2]^+$ , in the  
273 compounds. The absence of such O-species was shown with  $^{15}\text{N}$ -isotope labeling as besides the isotope-  
274 shifted  $\text{U}\equiv\text{N}$  band no  $\text{U}=\text{O}$  bands are observed in the Raman spectrum. Quantum chemical calculations  
275 showed that the chemical bonds in the  $[\text{UN}_2]$  moieties are best described with  $\text{U}\equiv\text{N}$  triple bonds.

276

## 277 **References**

- 278 1. Hunt, R. D., Yustein, J. T. & Andrews, L. Matrix infrared spectra of NUN formed by the  
279 insertion of uranium atoms into molecular nitrogen. *J. Chem. Phys.* **98**, 6070–6074  
280 (1993).
- 281 2. Wang, X., Andrews, L., Vlaisavljevich, B. & Gagliardi, L. Combined Triple and Double  
282 Bonds to Uranium: The  $\text{N}\equiv\text{U}=\text{N}-\text{H}$  Uranimine Nitride Molecule Prepared in Solid Argon.  
283 *Inorg. Chem.* **50**, 3826–3831 (2011).
- 284 3. Andrews, L. *et al.* Infrared Spectra and Electronic Structure Calculations for NN  
285 Complexes with U, UN, and NUN in Solid Argon, Neon, and Nitrogen. *J. Phys. Chem. A*  
286 **118**, 5289–5303 (2014).
- 287 4. Andrews, L., Wang, X., Gong, Y., Vlaisavljevich, B. & Gagliardi, L. Infrared Spectra and  
288 Electronic Structure Calculations for the  $\text{NUN}(\text{NN})_{1-5}$  and  $\text{NU}(\text{NN})_{1-6}$  Complexes in Solid  
289 Argon. *Inorg. Chem.* **52**, 9989–9993 (2013).
- 290 5. Falcone, M., Chatelain, L., Scopelliti, R., Živković, I. & Mazzanti, M. Nitrogen reduction  
291 and functionalization by a multimetallic uranium nitride complex. *Nature* **547**, 332–335  
292 (2017).

- 293 6. Cleaves, P. A. *et al.* Terminal Uranium(V/VI) Nitride Activation of Carbon Dioxide and  
294 Carbon Disulfide: Factors Governing Diverse and Well-Defined Cleavage and Redox  
295 Reactions. *Chem. Eur. J.* **23**, 2950–2959 (2017).
- 296 7. Falcone, M., Poon, L. N., Fadaei, T. F. & Mazzanti, M. Reversible Dihydrogen Activation  
297 and Hydride Transfer by a Uranium Nitride Complex. *Angew. Chem., Int. Ed.* **57**, 3697–  
298 3700 (2018).
- 299 8. Fox, A. R., Bart, S. C., Meyer, K. & Cummins, C. C. Towards uranium catalysts. *Nature*  
300 **455**, 341–349 (2008).
- 301 9. Fox, A. R., Arnold, P. L. & Cummins, C. C. Uranium–Nitrogen Multiple Bonding:  
302 Isostructural Anionic, Neutral, and Cationic Uranium Nitride Complexes Featuring a  
303 Linear U=N=U Core. *J. Am. Chem. Soc.* **132**, 3250–3251 (2010).
- 304 10. Rogozkin, B. D., Stepennova, N. M., Bergman, G. A. & Proshkin, A. A. Thermochemical  
305 Stability, Radiation Testing, Fabrication, and Reprocessing of Mononitride Fuel. *At.*  
306 *Energ.* **95**, 835–844 (2003).
- 307 11. Matthews, R. B., Chidester, K. M., Hoth, C. W., Mason, R. E. & Petty, R. L. Fabrication  
308 and testing of uranium nitride fuel for space power reactors. *J. Nucl. Mater.* **151**, 345–345  
309 (1988).
- 310 12. Diaconescu, P. Actinide chemistry: A tale of two nitrides. *Nat. Chem.* **2**, 705–706 (2010).
- 311 13. *Technology Roadmap Update for Generation IV Nuclear Energy Systems.* (2014).
- 312 14. King, D. M. *et al.* Isolation and characterization of a uranium(VI)–nitride triple bond. *Nat.*  
313 *Chem.* **5**, 482–488 (2013).
- 314 15. Gardner, B. M. *et al.* Triamidoamine uranium(IV)–arsenic complexes containing one-,  
315 two- and threefold U–As bonding interactions. *Nat. Chem.* **7**, 582–590 (2015).
- 316 16. Hayton, T. W. *et al.* Synthesis of Imido Analogs of the Uranyl Ion. *Science* **310**, 1941–  
317 1943 (2005).
- 318 17. King, D. M. & Liddle, S. T. Progress in molecular uranium-nitride chemistry. *Coord.*  
319 *Chem. Rev.* **266/267**, 2–15 (2014).

- 320 18. King, D. M. *et al.* Synthesis and Structure of a Terminal Uranium Nitride Complex.  
321 *Science* **337**, 717–720 (2012).
- 322 19. Camp, C., Pécaut, J. & Mazzanti, M. Tuning Uranium–Nitrogen Multiple Bond Formation  
323 with Ancillary Siloxide Ligands. *J. Am. Chem. Soc.* **135**, 12101–12111 (2013).
- 324 20. Evans, W. J., Kozimor, S. A. & Ziller, J. W. Molecular Octa-Uranium Rings with  
325 Alternating Nitride and Azide Bridges. *Science* **309**, 1835–1838 (2005).
- 326 21. Kushto, G. P., Souter, P. F. & Andrews, L. An infrared spectroscopic and quasirelativistic  
327 theoretical study of the coordination and activation of dinitrogen by thorium and uranium  
328 atoms. *J. Chem. Phys.* **108**, 7121–7130 (1998).
- 329 22. Andrews, L., Wang, X., Lindh, R., Roos, B. O. & Marsden, C. J. Simple  $N\equiv UF_3$  and  
330  $P\equiv UF_3$  Molecules with Triple Bonds to Uranium. *Angew. Chem., Int. Ed.* **47**, 5366–5370  
331 (2008).
- 332 23. Fox, A. R. & Cummins, C. C. Uranium–Nitrogen Multiple Bonding: The Case of a Four-  
333 Coordinate Uranium(VI) Nitridoborate Complex. *J. Am. Chem. Soc.* **131**, 5716–5717  
334 (2009).
- 335 24. Evans, W. J., Miller, K. A., Ziller, J. W. & Greaves, J. Analysis of Uranium Azide and  
336 Nitride Complexes by Atmospheric Pressure Chemical Ionization Mass Spectrometry.  
337 *Inorg. Chem.* **46**, 8008–8018 (2007).
- 338 25. Anderson, N. H. *et al.* Elucidating bonding preferences in tetrakis(imido)uranate(VI)  
339 dianions. *Nat. Chem.* **9**, 850–855 (2017).
- 340 26. Schmidt, A.-C., Heinemann, F. W., Maron, L. & Meyer, K. A Series of Uranium(IV, V, VI)  
341 Tritylimido Complexes, Their Molecular and Electronic Structures and Reactivity with  
342  $CO_2$ . *Inorg. Chem.* **53**, 13142–13153 (2014).
- 343 27. Rudel, S. S. *et al.* Recent advances in the chemistry of uranium halides in anhydrous  
344 ammonia. *Z. Kristallogr. - Cryst. Mater.* **233**, 817–844 (2018).
- 345 28. Jean-Claude Berthet, Gerald Siddredi, Pierre Thuery & Michel Ephritikhine. Synthesis  
346 and crystal structure of pentavalent uranyl complexes. The remarkable stability of  
347  $UO_2X$  ( $X = I, SO_3CF_3$ ) in non-aqueous solutions. *Dalton Trans.* 3478–3494 (2009).

- 348 29. Berthet, J.-C., Nierlich, M., Miquel, Y., Madic, C. & Ephritikhine, M. Selective  
349 complexation of uranium(III) over lanthanide(III) triflates by 2,2':6',2''-terpyridine. X-Ray  
350 crystal structures of  $[M(\text{OTf})_3(\text{terpy})_2]$  and  $[M(\text{OTf})_2(\text{terpy})_2(\text{py})][\text{OTf}]$  ( $M = \text{Nd}, \text{Ce}, \text{U}$ ) and  
351 of polynuclear  $\mu$ -oxo uranium(IV) complexes resulting from hydrolysis. *Dalton Trans.*  
352 369–379 (2005).
- 353 30. Fortier, S., Brown, J. L., Kaltsoyannis, N., Wu, G. & Hayton, T. W. Synthesis, Molecular  
354 and Electronic Structure of  $\text{U}^{\text{V}}(\text{O})[\text{N}(\text{SiMe}_3)_2]_3$ . *Inorg. Chem.* **51**, 1625–1633 (2012).
- 355 31. Gardner, B. M. *et al.* Homologation and functionalization of carbon monoxide by a  
356 recyclable uranium complex. *Proc. Natl. Acad. Sci. U. S. A.* **109**, 9265–9270 (2012).
- 357 32. Olovsson, I. The crystal structures of the triamines of the ammonium halides. *Acta*  
358 *Chem. Scand.* **14**, 1453–1465 (1960).
- 359 33. Olovsson, I. The Crystal Structure of Tetrammineammonium Iodide. *Acta Chem. Scand.*  
360 **14**, 1466–1474 (1960).
- 361 34. Roßmeier, T. Supramolekulare Chemie mit Ammoniak – Strukturchemie neuer  
362 Ammoniak-Proton-Komplexe. (Regensburg, 2005).
- 363 35. Roßmeier, T., Reil, M. & Korber, N. First Characterization of the Ammine–Ammonium  
364 Complex  $[\{\text{NH}_4(\text{NH}_3)_4\}_2(\mu\text{-NH}_3)_2]^{2+}$  in the Crystal Structure of  $[\text{NH}_4(\text{NH}_3)_4][\text{B}(\text{C}_6\text{H}_5)_4]\cdot\text{NH}_3$   
365 and the  $[\text{NH}_4(\text{NH}_3)_4]^+$  Complex in  $[\text{NH}_4(\text{NH}_3)_4][\text{Ca}(\text{NH}_3)_7]\text{As}_3\text{S}_6\cdot 2\text{NH}_3$  and  
366  $[\text{NH}_4(\text{NH}_3)_4][\text{Ba}(\text{NH}_3)_8]\text{As}_3\text{S}_6\cdot\text{NH}_3$ . *Inorg. Chem.* **43**, 2206–2212 (2004).
- 367 36. Roßmeier, T. & Korber, N. First Characterization of an Extended Ammonium-Ammonia  
368 Complex  $[\text{NH}_4(\text{NH}_3)_4^+(\mu\text{-NH}_3)_2]$  in the Crystal Structure of  
369  $[\text{NH}_4(\text{NH}_3)_4][\text{Co}(\text{C}_2\text{B}_9\text{H}_{11})_2]\cdot 2\text{NH}_3$ . *Z. Anorg. Allg. Chem.* **630**, 2665–2668 (2004).
- 370 37. Schmidt, K. H. & Müller, A. Vibrational Spectra and Force Constants of Pure Ammine  
371 Complexes. *Coord. Chem. Rev.* **19**, 41–97 (1976).
- 372 38. Wagner, W. D. & Nakamoto, K. Resonance Raman spectra of nitridoiron(V) porphyrin  
373 intermediates produced by laser photolysis. *J. Am. Chem. Soc.* **111**, 1590–1598 (1989).
- 374 39. Bullock, J. I. Raman and infrared spectroscopic studies of the uranyl ion: the symmetric  
375 stretching frequency, force constants, and bond lengths. *J. Chem. Soc. A* 781 (1969).

- 376 40. Nocton, G. *et al.* Synthesis, Structure, and Bonding of Stable Complexes of Pentavalent  
377 Uranyl. *J. Am. Chem. Soc.* **132**, 495–508 (2010).
- 378 41. Juza, R. & Meyer, W. Über Uran-Nitrid-Chlorid, -Bromid und -Jodid. *Z. Anorg. Allg.*  
379 *Chem.* **366**, 43–50 (1969).
- 380 42. Murasik, A., Furrer, A. & Szczepaniak, W. Crystal-field levels in UBr<sub>3</sub> determined by  
381 neutron spectroscopy. *Solid State Communications* **33**, 1217–1219 (1980).
- 382 43. Knizia, G. Intrinsic Atomic Orbitals: An Unbiased Bridge between Quantum Theory and  
383 Chemical Concepts. *J. Chem. Theory Comput.* **9**, 4834–4843 (2013).
- 384 44. Kaltsoyannis, N. Computational Study of Analogues of the Uranyl Ion Containing the  
385 –NUN– Unit: Density Functional Theory Calculations on UO<sub>2</sub><sup>2+</sup>, UON<sup>+</sup>, UN<sub>2</sub>, UO(NPH<sub>3</sub>)<sup>3+</sup>,  
386 U(NPH<sub>3</sub>)<sub>2</sub><sup>4+</sup>, [UCl<sub>4</sub>{NPR<sub>3</sub>}<sub>2</sub>] (R = H, Me), and [UOCl<sub>4</sub>{NP(C<sub>6</sub>H<sub>5</sub>)<sub>3</sub>}]<sup>-</sup>. *Inorg. Chem.* **39**,  
387 6009–6017 (2000).
- 388 45. Wei, F., Wu, G., Schwarz, W. H. E. & Li, J. Geometries, electronic structures, and excited  
389 states of UN<sub>2</sub>, NUO<sup>+</sup>, and UO<sub>2</sub><sup>2+</sup>: a combined CCSD(T), RAS/CASPT2 and TDDFT study.  
390 *Theor. Chem. Acc.* **129**, 467–481 (2011).

391

## 392 **Acknowledgement**

393 S.S. Rudel and F. Kraus thank the Deutsche Forschungsgemeinschaft for generous funding. A. J.  
394 Karttunen thanks CSC, the Finnish IT Center for Science, for computational resources. We thank Bernd  
395 Roling for using his Raman spectrometer. We thank Ulrich Müller to bring [UN<sub>2</sub>] to our attention many  
396 years ago.

397

## 398 **Author Contributions**

399 S.S.R. conceived and designed experiments, interpreted crystal structures, powder patterns and spectra  
400 on **1**<sup>8+</sup> and **3**<sup>6+</sup>. S.S.R. and M.M. performed experiments and analytics on **1**<sup>8+</sup> and **3**<sup>6+</sup>. M.M. contributed  
401 to the manuscript. H.L.D. conceived, designed and performed experiments on **2**<sup>7+</sup>. H.L.D. and M.M.



402 interpreted the single-crystal structure of  $2^{7+}$ . H.L.D. and M.M. contributed equally to the manuscript.  
403 A.J.K. conceived and designed the quantum chemical calculations, interpreted results, wrote the  
404 theoretical parts of the manuscript. F.K. designed and guided research, interpreted the single-crystal  
405 structure determinations, powder patterns, spectra. S.S.R. and F.K. wrote the manuscript. All authors  
406 discussed the results and commented on the manuscript.

407

## 408 Competing Interests Statement

409 The authors declare no competing interests.

410

## 411 Figure Legends

412 **Figure 1.** Representative Lewis structures and structures of the cations  $1^{8+}$ ,  $2^{7+}$ , and  $3^{6+}$  in their crystal structures,  
413 showing the central  $[N\equiv U\equiv N]$  units. L denotes  $NH_3$  ligands. U atoms are green, N atoms blue, Br atoms brown, and  
414 Cl atoms dark green. Anisotropic displacement ellipsoids are shown at 70 % probability level at 100 K. a) Cation  
415  $1^{8+}$ . b) Cations  $2^{7+}$ ; both crystallographically independent molecules are shown. The U–Br bonds are 2.9790(11)  
416 and 2.9689(11) Å in length. c) Cation  $3^{6+}$ . The U–Cl bonds are 2.8071(14) and 2.8365(14) Å in length.

417 **Figure 2.** Raman spectra of the compound  $2Br_7 \cdot 10.5NH_3$  with natural  $^{14}N/^{15}N$  isotope ratio and the isotope labelled  
418 compound with  $^{15}NH_3$ . a) Raman spectrum of the compound with  $NH_3$  in natural isotope ratio. b) Raman spectrum  
419 of the compound with  $^{15}N$  enriched ammonia. The bands in the range from circa 3158 to 3380  $cm^{-1}$  are assigned  
420 to symmetric and asymmetric N–H stretch vibrations of  $NH_3$  molecules, while the band at 906 (in a) and 883  $cm^{-1}$   
421 (in b) is assigned to the U–N and U– $^{15}N$  vibration within the central  $[UN_2]$  and  $[U^{15}N_2]$  moieties. The isotope shift is  
422 circa  $-23 cm^{-1}$ , ratio 1.026.

423 **Figure 3.** Intrinsic Bond Orbitals (IBOs) corresponding to the  $U\equiv N$  triple bonds in the  $[UN_2]$  molecule and cation  $1^{8+}$ .  
424 The red and green orbitals are the IBOs, while cyan, blue, and white denote U, N, and H atoms, respectively. a)  
425 shows the  $\sigma$ -bonds in  $[UN_2]$  and  $1^{8+}$ , b) shows the first set of  $\pi$ -bonds for  $[UN_2]$  and  $1^{8+}$ , and c) shows the second  
426 set of  $\pi$ -bonds. The listed percentages show the contribution of each atom in the IBO. In a purely covalent two-  
427 atomic bond, each atom would contribute 50%. The isovalue for IBO isosurface plots is 0.08 a.u.

428

## 429 Methods

430 All work was carried out under the exclusion of moisture and air in an atmosphere of dried and purified  
431 argon (Praxair 5.0, passed through titanium sponge at 800 °C) using vacuum glass lines or a glove box  
432 (MBraun). All glass vessels were flame dried under vacuum before use. Liquid ammonia (Air Liquide,  
433 99.98%) was dried and stored over sodium (VWR) in a special vacuum glass line.  $BCl_3$  (Merck, >99%)  
434 was distilled *in vacuo* and portioned into flame sealed glass ampoules. U turnings were washed with  
435 nitric acid, deionized and degassed water, then acetone, and dried in vacuum before use.  $Br_2$  was stirred

436 with P<sub>4</sub>O<sub>10</sub>, sublimed twice and stored over fresh P<sub>4</sub>O<sub>10</sub>. UF<sub>5</sub> was synthesized by the photoreduction of  
437 UF<sub>6</sub> with CO.<sup>46</sup> UCl<sub>5</sub> was synthesized by metathesis of UF<sub>5</sub> and BCl<sub>3</sub> in FEP-vessels which were dried  
438 in *in vacuo* at 100 °C.<sup>47</sup> UBr<sub>5</sub> was prepared from the elements.<sup>27,48</sup> The purity of both compounds was  
439 checked with powder X-ray diffraction, IR and Raman spectroscopy (Supplementary Figures 1-4).

440 **[U<sub>3</sub>(μ-N)<sub>2</sub>(NH<sub>3</sub>)<sub>21</sub>]Br<sub>8</sub>·26NH<sub>3</sub> (1Br<sub>8</sub>·26NH<sub>3</sub>), Henicosaammine-1κ<sup>8</sup>N,2κ<sup>8</sup>N,3κ<sup>5</sup>N-di-μ-**  
441 **nitrido-1:3κ<sup>2</sup>N;2:3κ<sup>2</sup>N-diuranium(4+)uranium(6+) bromide – ammonia(1/26)**

442 UBr<sub>5</sub> (220 mg, 0.35 mmol) was treated with liquid ammonia (~5 mL) inside a reaction tube at –78 °C.  
443 After two weeks of storage at –40 °C, green flat rod-shaped crystals of compound 1Br<sub>8</sub>·26NH<sub>3</sub> admixed  
444 with NH<sub>4</sub>Br and an unknown powder were obtained.

445 **[(NH<sub>3</sub>)<sub>8</sub>U(μ-N)Br(NH<sub>3</sub>)<sub>4</sub>U(μ-N)U(NH<sub>3</sub>)<sub>8</sub>]<sub>2</sub>Br<sub>14</sub>·21NH<sub>3</sub>, (2Br<sub>7</sub>·10.5NH<sub>3</sub>), Eicosaammine-**  
446 **1κ<sup>8</sup>N,2κ<sup>8</sup>N,3κ<sup>4</sup>N-bromido-3κ<sup>1</sup>Br-di-μ-nitrido-1:3κ<sup>2</sup>N;2:3κ<sup>2</sup>N-**  
447 **diuranium(4+)uranium(6+) bromide – ammonia(1/21)**

448 UBr<sub>5</sub> (15 mg, 0.024 mmol) was treated with liquid ammonia or <sup>15</sup>N-ammonia (~0.25 mL) inside a flame  
449 sealed silica ampoule (bomb tube, 4 mm outer diameter) for ten days at –35 °C. The bomb tube was  
450 sealed in vacuo at –196 °C. After three to four weeks of storage at room temperature green plate-shaped  
451 crystals of compound 2Br<sub>7</sub>·10.5NH<sub>3</sub> admixed with NH<sub>4</sub>Br were obtained.

452 **[U<sub>3</sub>Cl<sub>2</sub>(μ-N)<sub>2</sub>(NH<sub>3</sub>)<sub>19</sub>]Cl<sub>6</sub>·6NH<sub>3</sub>, (3Cl<sub>6</sub>·6NH<sub>3</sub>), Nonadecaammine-1κ<sup>8</sup>N,2κ<sup>8</sup>N,3κ<sup>3</sup>N-**  
453 **dichlorido-3κ<sup>2</sup>Cl-di-μ-nitrido-1:3κ<sup>2</sup>N;2:3κ<sup>2</sup>N-diuranium(4+)uranium(6+) chloride –**  
454 **ammonia(1/6)**

455 UCl<sub>5</sub> (33 mg, 0.08 mmol) was treated with liquid ammonia (~5 mL) in a flame sealed glass ampoule at  
456 –78 °C. The tube was sealed in vacuo at –196 °C. After six weeks of storage at room temperature green  
457 rod-shaped crystals of compound 3Cl<sub>6</sub>·6NH<sub>3</sub> and NH<sub>4</sub>Cl powder were obtained.

458 **Powder X-ray diffraction:** Powder X-Ray diffraction patterns were recorded inside flame sealed  
459 borosilicate glass capillaries by using a STOE Stadi MP powder diffractometer with germanium  
460 monochromated Cu<sub>Kα1</sub> radiation and a Mythen1K detector. Phase analysis was carried out with the  
461 WinXPOW software package.<sup>49</sup>

462 **Single-crystal X-ray analyses:** Single crystals were extracted from liquid ammonia at  $-78\text{ }^{\circ}\text{C}$ ,  
463 selected under exclusion of air in cooled perfluorinated polyether (Galden LS 230, Solvay Solexis) and  
464 mounted using the MiTeGen MicroLoop system. Data were collected at  $-173\text{ K}$  using a Stoe IPDS2/2T  
465 diffractometer with Mo- $K_{\alpha}$  ( $\lambda = 0.71073\text{ \AA}$ ) and processed with the Stoe X-Area software.<sup>50</sup> The  
466 diffraction data were scaled with the Laue Analyzer in X-Area and corrected for absorption with the X-  
467 Red and X-Shape software.<sup>51-53</sup> The structures were solved by using Direct Methods (SHELXS-97  
468 ( $1\text{Br}_8 \cdot 26\text{NH}_3$ ) and SHELXT-14/5 ( $2\text{Br}_7 \cdot 10.5\text{NH}_3$ ,  $3\text{Cl}_6 \cdot 6\text{NH}_3$ ))<sup>54,55</sup> and refined against  $F^2$  (SHELXL-  
469 2016/6)<sup>56</sup> using the ShelXle software package.<sup>57</sup> The crystal structure of  $1\text{Br}_8 \cdot 26\text{NH}_3$  contains a large  
470 amount of ammonia of crystallization. We refined the nitrogen atoms of the ammonia molecules of  
471 solvation N47 to N49 as split positions and N48 and N49 with the SUMP command, as these atoms are  
472 heavily disordered inside channels along the  $c$  axis at  $z = 1/2$ . For the ammonia molecules, located on  
473 split positions, as well as those with the nitrogen atoms N38, N42, N43, N46, the H atoms could not be  
474 located from the electron density map.

475 **IR Spectroscopy:** IR Spectra were recorded by using the PLATINUM ATR module on a Bruker  
476 Alpha FT-IR spectrometer with a spectral resolution of  $4\text{ cm}^{-1}$  inside a glovebox. The data were treated  
477 with the OPUS software package and Origin 2017.<sup>58</sup>

478 **Raman Spectroscopy:** Raman spectra were recorded for  $1\text{Br}_8 \cdot 26\text{NH}_3$  and  $3\text{Cl}_6 \cdot 6\text{NH}_3$  with a  
479 Renishaw Raman microscope, using a frequency-doubled Nd:YAG Laser (532 nm wavelength). For  
480  $2\text{Br}_7 \cdot 10.5\text{NH}_3$ , the Raman spectra were measured at room temperature with a Monovista CRS+ confocal  
481 Raman microscope (Spectroscopy & Imaging GmbH) using a 532 nm solid-state laser. We reacted  $\text{UBr}_5$   
482 and  $\text{UCl}_5$ , respectively, inside a flame-sealed fused silica tube with 0.5 mm wall thickness and 4 mm  
483 diameter. One sample of  $\text{UBr}_5$  in ammonia was kept at  $-36\text{ }^{\circ}\text{C}$  until the measurement. The other samples  
484 were stored at room temperature for three days. Crystals, precipitated powder as well as the solutions,  
485 were subjected to Raman spectroscopy inside these tubes under the pressure of liquid ammonia at room  
486 temperature.

487 **Computational details:** Quantum chemical calculations were carried out using the TURBOMOLE  
488 program package.<sup>59,60</sup> We used the PBE0 hybrid density functional method and a triple-zeta-valence  
489 quality basis set with polarization functions (def-TZVP).<sup>61-64</sup> Scalar relativistic effects were taken into  
490 account by applying a 60-electron relativistic effective core potential for U.<sup>65</sup> Multipole-accelerated  
491 resolution-of-the-identity technique was used to speed up the calculations.<sup>66-68</sup> Cations **1-3** were fully  
492 optimized without any symmetry constraints ( $C_1$  point group), cartesian coordinates are available in  
493 Source Data 2.  $[\text{UN}_2(\text{NH}_3)_5]$  and  $[\text{UO}_2(\text{NH}_3)_5]^{2+}$  were optimized in the  $C_{5h}$  point group, while for  $[\text{UN}_2]$   
494 and  $[\text{UO}_2]^{2+}$ , the  $D_{6h}$  point group was applied. Because the molecular calculations of the cations **1-3** lack  
495 the counteranions present in the solids, we applied the COSMO continuum solvation model to counter  
496 the rather high positive charge of the cations.<sup>69</sup> Harmonic frequency calculations were carried out on the  
497 optimized structures. For **1**<sup>8+</sup>, two imaginary frequencies corresponding to rotational motion of two  
498 ammonia ligands persisted even after several re-optimizations carried out by following the imaginary  
499 modes ( $350i$  and  $224i$   $\text{cm}^{-1}$ ). The imaginary modes probably arise because the highly charged (8+) cation  
500 has been cut out from the crystal field and embedded in a COSMO solvent field. Cations **2**<sup>7+</sup> and **3**<sup>6+</sup>  
501 with slightly lower charge do not show any imaginary modes. Molecular  $[\text{UN}_2]$ ,  $[\text{UO}_2]^{2+}$ ,  $[\text{UN}_2(\text{NH}_3)_5]$   
502 and  $[\text{UO}_2(\text{NH}_3)_5]^{2+}$  were also confirmed to be true local minima. In the Raman spectrum calculations ( $\lambda$   
503 = 532 nm; T = 298.15 K, unpolarized radiation, scattering angle of  $90^\circ$ ),<sup>70</sup> the COSMO solvent model  
504 was not used in the calculation of the ground state or the dynamic polarizability derivatives. The Raman  
505 intensities are given relative to the most intensive peak. The final Raman spectra were convoluted using  
506 Lorentzian peak profiles with FWHM of  $20$   $\text{cm}^{-1}$ . Intrinsic Atomic Orbitals (IAOs) and Bond Orbitals  
507 (IBOs) were used in the bonding analysis.<sup>43,71</sup> For the IAO and IBO analysis of uranium, we used free-  
508 atom reference orbitals that are described in Source Data 1.

#### 509 **Additional details for the IBO reference orbitals**

510 Like molecular orbitals, IBOs are not physical observables, but they can be considered as a physically  
511 well-defined form of localized molecular orbitals (MOs) designed for chemical interpretation.<sup>43,71</sup> While  
512 delocalized canonical molecular orbitals are often difficult to connect to textbook-level chemical  
513 concepts, IBOs are a powerful technique to represent wavefunctions in an exact and a simple way.

514 The listed percentages (Figure 3, Supplementary Table 4, Extended Data Fig. 5) show the contribution  
515 of each atom in the IBO (if the percentages do not add up exactly to 100%, some other atoms are giving  
516 minor contributions smaller than 1%). The interpretation of the IBOs is rather simple: In a purely  
517 covalent two-atomic bond, each atom would contribute 50%. The further the contributions differ from  
518 50%, the more ionic the bond is. There can also be some minor contributions from other atoms.

519 Generation of IBOs requires a set of reference orbitals that have been obtained for an isolated atom and  
520 Knizia proposed to derive the reference orbitals from the triple-zeta-valence cc-pVTZ basis set.<sup>43,71</sup> The  
521 TURBOMOLE basis set library includes IBO reference orbitals based on cc-pVTZ or cc-pVTZ-PP basis  
522 sets for most elements, but there are no reference orbitals for uranium. We derived a set of reference  
523 orbitals for the uranium  $5f^36d^17s^2$  ground state (Restricted-Open HF with Roothaan parameters  $a =$   
524  $21/26$ ,  $b = 21/26$ ). The reference orbitals (TURBOMOLE format, Supplementary Data 4) were obtained  
525 for the def-TZVP basis set (without polarization functions).<sup>63,64</sup> We also checked that the IBO results  
526 were similar with reference orbitals obtained for the uranium cc-pVTZ-PP basis set.

527

## 528 **References for methods section**

- 529 27. Rudel, S. S. *et al.* Recent advances in the chemistry of uranium halides in anhydrous  
530 ammonia. *Z. Kristallogr. - Cryst. Mater.* **233**, 817–844 (2018).
- 531 46. Scheibe, B., Rudel, S. S., Buchner, M. R., Karttunen, A. J. & Kraus, F. A 1D Coordination  
532 Polymer of  $UF_5$  with HCN as a Ligand. *Chem. - Eur. J.* **23**, 291–295 (2017).
- 533 47. Brown, D., Berry, J. A. & Holloway, J. H. Halogen exchange reactions involving uranium-  
534 (V) and -(VI) halides. *J. Chem. Soc., Dalton Trans.* 1385–1388 (1982).
- 535 48. Deubner, H. L. *et al.* A Revised Structure Model for the  $UCl_6$  Structure Type, Novel  
536 Modifications of  $UCl_6$  and  $UBr_5$ , and a Comment on the Modifications of Protactinium  
537 Pentabromides. *Chem. Eur. J.* **25**, 6402–6411 (2019).
- 538 49. *STOE WinXPOW*. (STOE & Cie GmbH, 2015); <https://www.stoe.com/>
- 539 50. *X-Area*. (STOE & Cie GmbH, 2018); <https://www.stoe.com/>
- 540 51. *X-RED32*. (STOE & Cie GmbH, 2012); <https://www.stoe.com/>

- 541 52. X-SHAPE. (STOE & Cie GmbH, 2013); <https://www.stoe.com/>
- 542 53. LANA - Laue Analyzer. (STOE & Cie GmbH, 2019); <https://www.stoe.com/>
- 543 54. Sheldrick, G. M. SHELXS-97. (1997); <http://shelx.uni-ac.gwdg.de/SHELX/index.php>
- 544 55. Sheldrick, G. M. SHELXT – Integrated space-group and crystal-structure determination.
- 545 *Acta Crystallogr., Sect. A: Found. Adv.* **71**, 3–8 (2015).
- 546 56. Sheldrick, G. M. SHELXL-2016/6. (2016); <http://shelx.uni-ac.gwdg.de/SHELX/index.php>
- 547 57. Hübschle, C. B., Sheldrick, G. M. & Dittrich, B. ShelXle: a Qt graphical user interface for
- 548 SHELXL. *J. Appl. Crystallogr.* **44**, 1281–1284 (2011).
- 549 58. OPUS. (Bruker Optik GmbH, 2009); <https://www.bruker.com/>
- 550 59. Ahlrichs, R., Bär, M., Häser, M., Horn, H. & Kölmel, C. Electronic structure calculations
- 551 on workstation computers: The program system turbomole. *Chem. Phys. Lett.* **162**, 165–
- 552 169 (1989).
- 553 60. Turbomole versions 7.2 and 7.3. University of Karlsruhe and Forschungszentrum
- 554 Karlsruhe GmbH. TURBOMOLE. (TURBOMOLE GmbH, 2017);
- 555 <http://www.turbomole.com>
- 556 61. Perdew, J. P., Burke, K. & Ernzerhof, M. Generalized Gradient Approximation Made
- 557 Simple. *Phys. Rev. Lett.* **77**, 3865–3868 (1996).
- 558 62. Adamo, C. & Barone, V. Toward reliable density functional methods without adjustable
- 559 parameters: The PBE0 model. *J. Chem. Phys.* **110**, 6158–6170 (1999).
- 560 63. Schäfer, A., Huber, C. & Ahlrichs, R. Fully optimized contracted Gaussian basis sets of
- 561 triple zeta valence quality for atoms Li to Kr. *J. Chem. Phys.* **100**, 5829–5835 (1994).
- 562 64. Cao, X. & Dolg, M. Segmented contraction scheme for small-core actinide
- 563 pseudopotential basis sets. *J. Mol. Struct.: THEOCHEM* **673**, 203–209 (2004).
- 564 65. W. Küchle, M. Dolg, H. Stoll & H. Preuss. Energy-adjusted pseudopotentials for the
- 565 actinides. Parameter sets and test calculations for thorium and thorium monoxide. *J.*
- 566 *Chem. Phys.* **100**, 7535–7542 (1994).
- 567 66. Eichkorn, K., Treutler, O., Öhm, H., Häser, M. & Ahlrichs, R. Auxiliary basis sets to
- 568 approximate Coulomb potentials. *Chem. Phys. Lett.* **240**, 283–290 (1995).

- 569 67. Weigend, F. Accurate Coulomb-fitting basis sets for H to Rn. *Phys. Chem. Chem. Phys.*  
570 **8**, 1057–1065 (2006).
- 571 68. Sierka, M., Hogekamp, A. & Ahlrichs, R. Fast evaluation of the Coulomb potential for  
572 electron densities using multipole accelerated resolution of identity approximation. *J.*  
573 *Chem. Phys.* **118**, 9136–9148 (2003).
- 574 69. Klamt, A. & Schürmann, G. COSMO: a new approach to dielectric screening in solvents  
575 with explicit expressions for the screening energy and its gradient. *J. Chem. Soc., Perkin*  
576 *Trans.* **2** 799–805 (1993).
- 577 70. Rappoport, D. & Furche, F. Lagrangian approach to molecular vibrational Raman  
578 intensities using time-dependent hybrid density functional theory. *J. Chem. Phys.* **126**,  
579 201104 (2007).
- 580 71. Knizia, G. & Klein, J. E. M. N. Electron Flow in Reaction Mechanisms—Revealed from  
581 First Principles. *Angew. Chem. Int. Ed.* **54**, 5518–5522 (2015).

582

### 583 **Data availability statement**

584 Crystal Structure Data were deposited with [The Cambridge Crystallographic Data Centre](#) (depository  
585 numbers 1868199 for  $3\text{Cl}_6 \cdot 6\text{NH}_3$ , 1868200 for  $1\text{Br}_8 \cdot 26\text{NH}_3$ , 1984956 for  $2\text{Br}_7 \cdot 10.5\text{NH}_3$ ) and within  
586 the Supplementary Information. Powder X-ray patterns, Raman and IR spectra and details of the  
587 quantum chemical calculations are in the Supplementary Information.

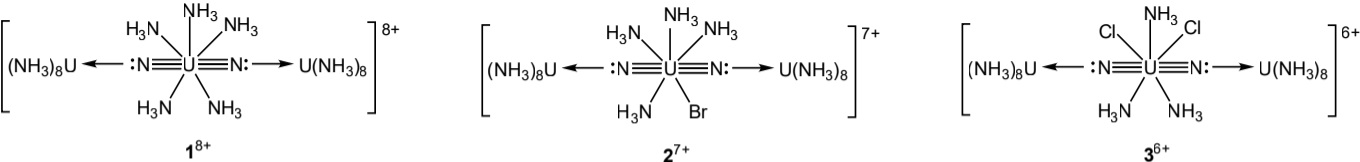


Figure 1

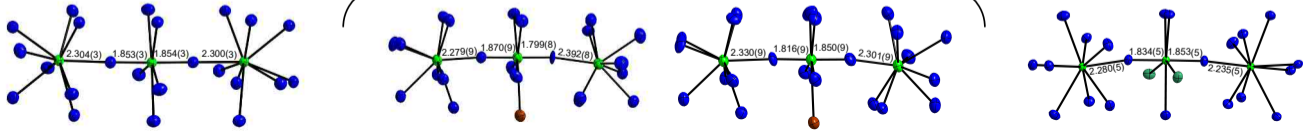




Figure 2

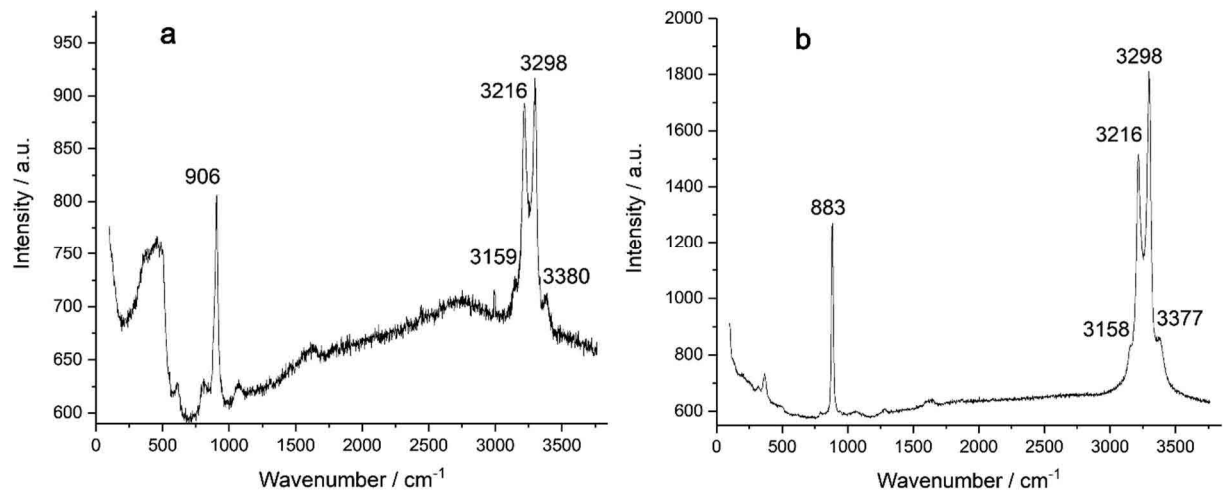
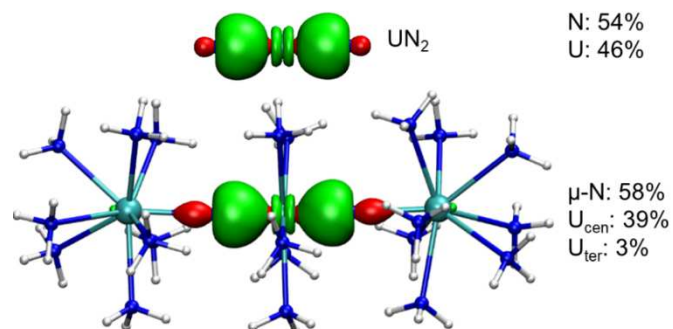
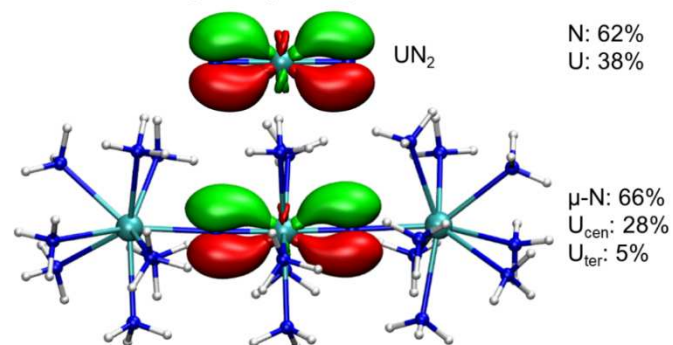


Figure 3

**a** Two  $\sigma$ -bonding IBOs



**b** Two  $\pi$ -bonding IBOs (first set)



**c** Two  $\pi$ -bonding IBOs (second set)

